Supporting Information

Stackable nickel-cobalt@polydopamine nanosheet based photothermal sponges for highly efficient solar steam generation

Bo Shao,[1] Yida Wang,[1] Xuan Wu,[1] Yi Lu,[2] Xiaofei Yang,[2] George Y. Chen,[3] Gary Owens,[1] Haolan Xu[1,*]

[1]Future Industries Institute, University of South Australia, Mawson Lakes Campus, SA 5095, Australia

[2] College of Science, Nanjing Forestry University, Nanjing, 210037, China

[3] School of Engineering, University of South Australia, Mawson Lakes Campus, SA 5095, Australia

Experimental section

Synthesis of Ni_1Co_3 nanosheets: $NiCl_2{\cdot}6H_2O$ and $CoCl_2{\cdot}6H_2O$ at a molar ration of 1:3 (50 mg: 150 mg) were dissolved in 100 mL of Millipore water and the solution was kept stirring. Then 30 mL of $NaBH_4$ (0.1 M) solution was slowly added into the above solution. The reaction solution was sealed for 8 h. The black resultant precipitates were collected and washed by ethanol and water several times.

Synthesis of Ni_1Co_3@PDA nanosheets: To form a PDA layer on the surface of the Ni_1Co_3 nanosheets, the obtained Ni_1Co_3 nanosheets were redispersed into dopamine hydrochloride (2 mg mL^{-1}) Tris buffer solution (pH = 8.5, 50 m M) with $CuSO_4$ (5 m M) and H_2O_2 (19.6 × m M) for 1 h, followed by centrifugation and washing with water for several times.

Preparation of Ni_1Co_3@PDA-based photothermal sponges: 500 mg of Ni_1Co_3@PDA nanosheets and 50 mg of SA (5mg/mL) were dispersed into 10 mL water and was kept stirring at room temperature for 6 hours to obtain a homogeneous solution. The obtained solution was then poured onto a circular piece of sponge (3.1 cm in diameter and 0.6 cm in thickness). The resulting sample was then allowed gelation for 2 hours and pre-frozen at -22 ^oC for 12 hours. Afterward, the obtained Ni_1Co_3@PDA-sponge was freeze-dried at -60 ^oC to obtain the Ni_1Co_3@PDA-based photothermal sponge.

Characterization: Field emission scanning electron microscopy (SEM) images were recorded using a Zeiss Merlin SEM. UV-Vis spectrum were recorded on a UV-2600 Spectrophotometer (Shimadzu). Infrared photographs were taken using an IR camera (FLIRE64501). Seawater

was collected from Semaphore Beach, Adelaide, Australia. The salinity of the seawater was measured using an Inductively Coupled Plasma Optical Emission Spectrometry (ICP-OES, Optima 5300V, Perkin Elmer). After solar evaporation, the ion concentrations of the collected water were measured using an ICP Triple Quad system (ICP-QQQ, Agilent 8800).

Water Evaporation Tests: Milli-Q water or seawater was held in a 200 mL plastic bottle. A polystyrene (PS) foam collar with a hole (3.1 cm in diameter) was employed as a cap for the bottle and to hold the cotton rod which served as a 1D water path. The Ni_1Co_3@PDA-based photothermal sponges were then placed on the top of the cotton rod. The other end of the cotton rod was immersed in the bulk water so that the water could continuously be transferred to the Ni_1Co_3@PDA-based photothermal sponges by capillary action. Simulated sunlight was provided by a Newport Oriel Solar Simulator (Newport Oriel Xenon Lamp, 66485-300XF-R1). The plastic bottle was placed on an electronic balance that was connected to a computer to monitor the water mass loss in real time.

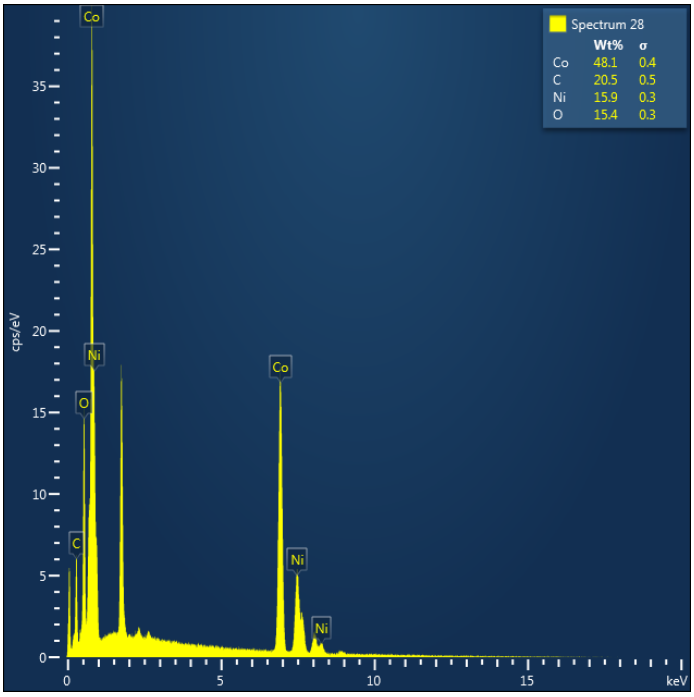

Fig. S1 EDX spectrum of the Ni_1Co_3 bimetal. The weight ratio of Ni:Co is 48.1:15.9, corresponding to an atomic ratio of 1:3.01.

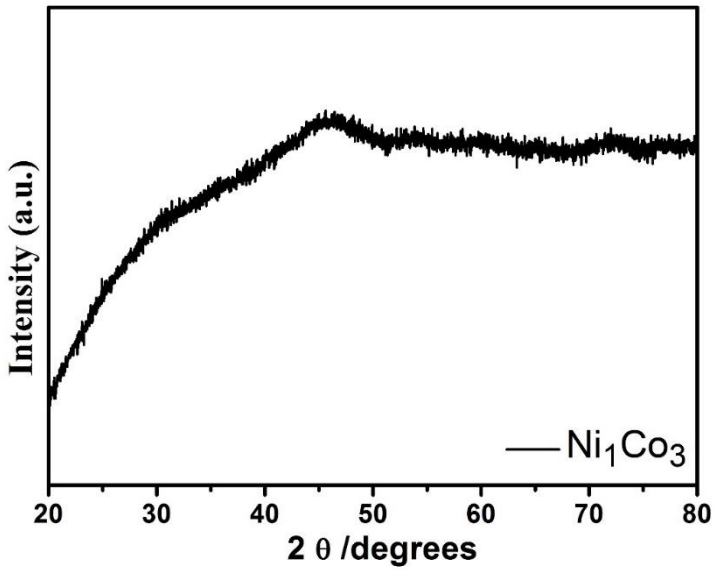

Fig. S2 XRD pattern of Ni_1Co_3 nanosheets. The broad weak peak over a wide 2θ range (42 - 48°) with no other clear peaks indicated that the obtained Ni_1Co_3 was amorphous.

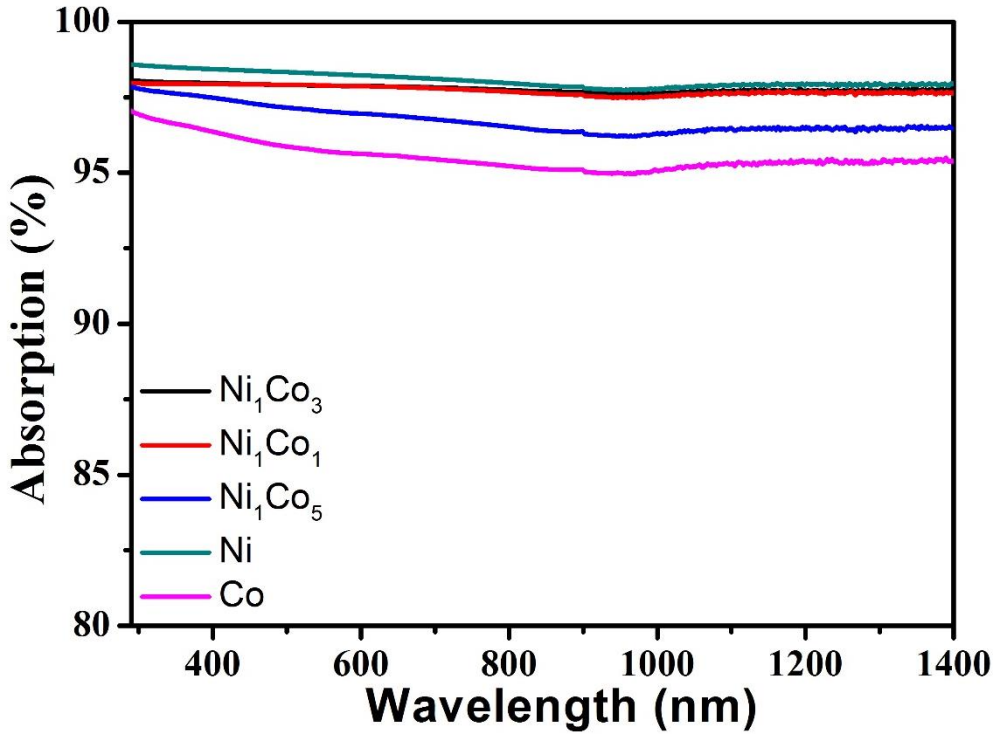

Fig. S3 UV-Vis spectra of Ni-Co bimetals without PDA coating.

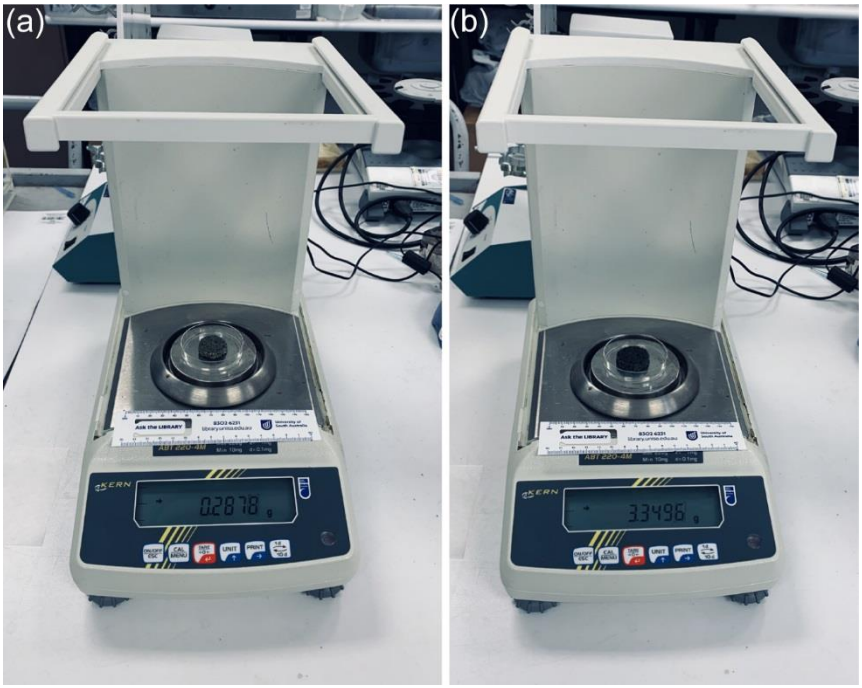

Fig. S4 Digital photographs illustrating weight change in photothermal sponge (a) before and (b) after water uptake.

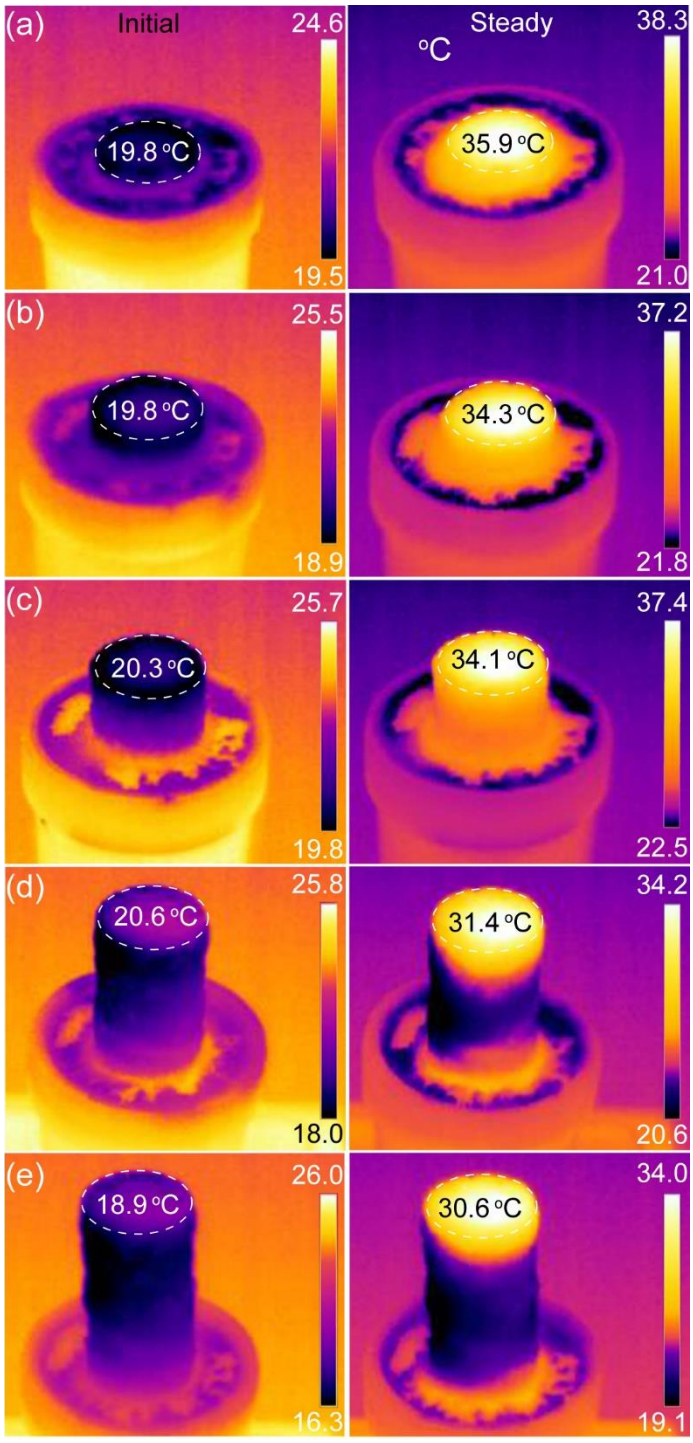

Fig. S5 IR images showing the initial and steady average top surface temperatures of the photothermal sponges with heights of (a) 0.6 cm, (b) 1.2 cm, (c) 2.4 cm, (d) 4.8 cm and (e) 6.0 cm.

Table S1 The comparison of photothermal evaporation performance for Ni_1Co_3@PDA sponge and the reported photothermal materials and evaporators

Photothermal materials/evaporator	Structure	Light intensity (kW/m^2)	Evaporation rate (kg/m^2h)	Publication
Ni_1Co_3@PDA sponge	3D	1.0	2.42	This work
Ni-NiO_x/Ni foam	2D	1.0	1.41	J. Mater. Chem. A, 2019, 7, 8485
Al nanoparticles/AAM	2D	1.0	0.92	Nat. Photonics 2016, 10, 393
Semiconductor particles-based cup shaped structure	3D	1.0	2.04	Joule 2018, 2, 1171
Carbonized mushrooms	3D	1.0	1.48	Adv. Mater. 207, 29, 1606762
Carbonized sunflower heads	3D	1.0	1.51	ACS Appl. Mater. Interfaces 2020, 12, 2171
CuS based aerogel	3D	1.0	1.63	Nano Energy, 2019, 56, 708
Carbon black-based cylinder structure	3D	1.0	1.62	Joule 2018, 2, 1331
Nanoink-stained sponge	3D	1.0	2.15	Nano Energy, 2019, 55, 368
Graphene oxide-based umbrella structure	3D	1.0	1.80	Natl. Sci. Rev. 2018, 5, 70
Carbon felt-based Hierarchical Structure	3D	1.0	1.56	ACS Appl. Mater. Interfaces 2019, 11, 32038
Carbonized carrot	3D	1.0	2.04	J. Mater. Chem. A, 2019, 7, 26911
Graphite paper-based origami structure	3D	1.0	1.16	Chem. Eng. J. 2019, 356, 869
$CuFeMnO_4$ coated honeycomb ceramic	3D	1.0	1.45	Nano Energy 2019, 60, 222
Carbon nanotube-based 3D printed cone structure	3D	1.0	2.63	Nature Communication 2020, 11, 521
Reduced graphene oxide and rice straw fiber-based cylinder aerogel	3D	1.0	2.25	ACS Appl. Mater. Interfaces 2020, 12, 15279

Energy calculation:

To explain the extremely high energy efficiency, energy exchange between the photothermal sponges and the environment was analysed using the following equation:

$$E_{\text{environment}} = A_1\varepsilon\sigma\left({T_1}^4 - {T_0}^4\right) + A_2\varepsilon\sigma\left({T_2}^4 - {T_0}^4\right) + A_1h(T_1 - T_0) + A_2h(T_2 - T_0) + q_{\text{water}} - q_{other}$$

For the 0.6 cm sample, A_1 is the area of the top surface of the photothermal sponge (7.55 cm^2), T_1 is the average surface temperature of the top surface (~35.9 °C), A_2 is the side surface area (5.843 cm^2), and T_2 is the average surface temperature of the side wall (~ 32.3 °C), T_0 is the ambient temperature (25 °C), ε is emissivity of the absorbing surface (~0.90), σ is the Stefan–Boltzmann constant (5.67× 10^{-8} Wm^{-2} K^{-4}), h is the convection heat transfer coefficient (assumed to be 5 W m^{-2} K^{-1}), and q_{water} is the energy exchange between the stored water and the photothermal sponge, which is 0 W in this work.

According to the above equation, for the 0.6 cm photothermal sponge, the radiation loss from the top evaporation surface was estimated to be 0.0470 W, while radiation energy loss of the side evaporation surface was 0.0239 W. Convection loss from the top evaporation surface was estimated to be 0.0411 W, and convection energy loss of the side evaporation surface was estimated to be 0.0210 W. The total energy loss was 0.133 W.

For the 6.0 cm sample, A_1 is 7.55 cm^2, T_1 is 31.1 °C, A_2 is 58.43 cm^2, and T_2 is 23.6 °C, T_0 is the ambient temperature (25 °C), ε is emissivity of the absorbing surface (~0.90), σ is the Stefan–Boltzmann constant (5.67× 10^{-8} Wm^{-2} K^{-4}), h is convection heat transfer coefficient (assumed to be 5 W m^{-2} K^{-1}), and q_{water} is is the energy exchange between the stored water and the photothermal sponge, which is 0 W in this work. Since the side evaporation surface has a lower temperature than the environment temperature ($T_2 < T_0$), it could gain energy from the environment.

According to the above equation, for the 6.0 cm photothermal sponge, the radiation loss from the top evaporation surface was estimated to be 0.0256 W, while radiation energy gain of the side evaporation surface from surrounding environment was 0.0438 W. Convection loss from the top evaporation surface was estimated to be 0.0237 W, and convection energy gain of the side evaporation surface from surrounding environment was estimated to be 0.0354 W. Therefore, the evaporator has a net energy gain of 0.0792 W from the environment.